Stochastic Model for Time-Varying Millimeter-Wave Beam Gains with User Orientation Changes

Ashok Kumar Reddy Chavva, *Senior Member, IEEE* and Neelesh B. Mehta, *Fellow, IEEE*

***Abstract*—In the widely used spatial channel model (SCM), the millimeter wave channels encountered by a 5G system are constructed using a stochasto-geometric approach. However, a probabilistic characterization of the time evolution of the gain of any transmit-receive beam pair is not available. We propose a novel modified bivariate Nakagami-m (MBN) model that presents such a characterization. It accurately captures the non-stationary time-variation in the beam gain due to user mobility and user device orientation changes. It applies to both positive and negative correlations between the beam gains. We derive closed-form expressions for the MBN parameters in terms of the SCM parameters. We then apply this tractable model to develop a new, effective, and robust beam selection rule. It predicts in closed-form the signal-to-noise ratios of the beam pairs at the time a beam pair is selected given the beam pair gain measurements that are made at different times.**

I. Introduction

5G cellular communication technology has moved towards millimeter-wave bands, where larger bandwidths are available [1]. To overcome the severe propagation loss in these bands, it employs high-gain narrow beams. As a result, many transmit-receive beam pairs are needed to cover the complete angular space. Thus, beam acquisition, which sounds the channel using different transmit-receive beam pairs at different times to determine the best transmit-receive beam pair, can take a considerable amount of time. Consequently, gain estimates for different beam pairs are outdated by different extents in a time-varying environment. In addition to user mobility, changes in the user equipment (UE) device orientation cause these variations. They also lead to beam misalignment and can make the channel non-stationary [2], [3].

User mobility and user orientation changes make it necessary to periodically reselect the transmit and receive beam pair. For this, it is important to periodically estimate the beam gains of the different beam pairs and also predict their evolution until the time instant at which the beam pair is selected. Prediction requires an accurate statistical model for the time evolution of the beam gain of every beam pair. Specifically, it requires the multivariate probability distribution of the beam gains of a beam pair at two or more time instants.

The time evolution of the beam gain is captured in a different stochasto-geometric manner in the spatial channel model (SCM), which has been used extensively in the third generation partnership project (3GPP) to evaluate 5G technologies [4]. SCM is based on real-world channels measured in many environments. It constructs the multiple-input-multiple-output (MIMO) channel matrix by summing over the contributions from different clusters, each of which consists of multiple paths. This combined with the transmit and receive array gain vectors, which depend on the beam pair, determines the gain of the beam pair. However, SCM does not provide a statistical model for the gain of a beam pair at one or more instants.

Ashok Kumar Reddy Chavva is with the Samsung Research Institute, Bangalore, India and Neelesh B. Mehta is with the Department of Electrical Communication Engineering (ECE), Indian Institute of Science (IISc), Bangalore, India (emails: ashok.chavva@samsung.com, nbmehta@iisc.ac.in).

A. Contributions

We first show empirically that, in SCM, the beam gains at two time instants can be positively or negatively correlated. Negative correlation occurs, for example, for a beam that is losing alignment between the first and second time instants. We then propose a novel bivariate Nakagami-m (MBN) model to accurately model the joint statistics of the gains of a beam pair at any two time instants for positive and negative correlations.

For the positively correlated case, it models the joint probability density function (PDF) of the two beam gains using the bivariate Nakagami-m model, which is known to accurately model the channel measurements obtained from several propagation scenarios. We derive closed-form expressions for the mean beam power, power correlation coefficient, and Nakagami parameter m in terms of the SCM parameters. While the Nakagami-m model is a classical channel model, its bivariate PDF for modeling the time-varying millimeter-wave channels of SCM and the effect of user orientation changes has not been employed in the literature, nor has its accuracy been verified. The expressions for its parameters are also novel.

Second, for negatively correlated beam gains, for which the conventional bivariate Nakagami-m PDF is not defined, MBN employs a novel bivariate PDF. The PDF is obtained by means of an affine transformation of the bivariate Nakagami-m PDF. We numerically verify the accuracy of the MBN model for both positive and negative correlations.

To demonstrate the MBN model's utility and tractability, we then apply it to improve the accuracy of beam selection. For a general beam selection model, in which a beam pair is selected periodically on the basis of the beam gain estimates that are outdated by different extents, we propose a new beam selection rule. It employs the MBN model to predict the signal-to-noise ratio (SNR) at the time of beam selection. It differs from the prevalent approach in the literature in which the beam pair with the largest measured signal power is selected [5]–[7].

B. Outline and Notation

Section II presents the system model. In Section III, we propose the MBN model and verify its accuracy. We apply

GLOBECOM 2021 - 2021 IEEE Global Communications Conference | 978-1-7281-8104-2/21/$31.00 ©2021 IEEE | DOI: 10.1109/GLOBECOM46510.2021.9685581

the MBN model to improve beam selection in Section IV. Our conclusions follow in Section V.

Notation: We denote the PDF and cumulative distribution function (CDF) of a random variable (RV) X by $f_X(\cdot)$ and $F_X(\cdot)$, respectively. Similarly, the conditional PDF and CDF conditioned on an event A are denoted by $f_X(\cdot|A)$ and $F_X(\cdot|A)$, respectively. The expectation with respect to an RV X is denoted by $\mathbb{E}_X[\cdot]$, and the expectation conditioned on an event A by $\mathbb{E}_X[\cdot|A]$. The covariance of RVs X and Y is denoted by $\mathrm{Cov}(X,Y)$, variance by $\mathrm{Var}(\cdot)$, transpose by $(\cdot)^T$, Hermitian transpose by $(\cdot)^\dagger$, and real part by $\Re\{\cdot\}$.

II. System Model

We consider a millimeter-wave system in which the base station (BS) is equipped with a uniform linear array (ULA) that consists of N_{tx} antennas. It can transmit on one beam from among B_{BS} fixed directional beams in the azimuth direction. Similarly, the UE is equipped with a ULA that consists of N_{rx} antennas. It can receive on one beam from among B_{UE} fixed directional beams in the azimuth direction. Let $\mathcal{B}_{\text{BS}} = \{1,\ldots,B_{\text{BS}}\}$ and $\mathcal{B}_{\text{UE}} = \{1,\ldots,B_{\text{UE}}\}$ denote the set of transmit and receive beams, respectively.

SCM: Let $\psi(t)$ be the orientation of the UE with respect to its antenna array at time t. As per SCM, the $N_{\text{rx}} \times N_{\text{tx}}$ MIMO baseband channel matrix $\mathbf{H}(t,\psi(t))$ between the BS and the UE at time t with UE orientation $\psi(t)$ is [4]

$$\mathbf{H}(t,\psi(t)) = \sqrt{\frac{K\Lambda}{K+1}}\mathbf{u}_{\text{rx}}(\theta^{\text{rx}}_{\text{LoS}}+\psi(t))\mathbf{u}^\dagger_{\text{tx}}(\theta^{\text{tx}}_{\text{LoS}}) + \sqrt{\frac{\Lambda}{(K+1)L}}\sum_{c=1}^{C}\sum_{l=1}^{L}\alpha_{c,l}(t)\mathbf{u}_{\text{rx}}(\theta^{\text{rx}}_{c,l}+\psi(t))\mathbf{u}^\dagger_{\text{tx}}(\theta^{\text{tx}}_{c,l}), \quad (1)$$

where C is the number of clusters, L is the number of paths per cluster, $\mathbf{u}_{\text{rx}}(\cdot)$ is the array response at the receiver, $\mathbf{u}_{\text{tx}}(\cdot)$ is the array response at the transmitter, K is the Rician factor, $\theta^{\text{tx}}_{c,l}$ and $\theta^{\text{rx}}_{c,l}$ are the angle of departure (AoD) at the BS and angle of arrival (AoA) at the UE, respectively, for the l^{th} path in the c^{th} cluster, $\theta^{\text{tx}}_{\text{LoS}}$ is the line-of-sight (LoS) AoD, $\theta^{\text{rx}}_{\text{LoS}}$ is the LoS AoA, and Λ is the path-loss. For a ULA,

$$\mathbf{u}_{\text{rx}}(\theta) = \frac{1}{\sqrt{N_{\text{rx}}}}\left[1, e^{-j2\pi\mu^{\text{rx}}(\theta)},\ldots,e^{-j2\pi(N_{\text{rx}}-1)\mu^{\text{rx}}(\theta)}\right]^T,$$
$$\mathbf{u}_{\text{tx}}(\theta) = \frac{1}{\sqrt{N_{\text{tx}}}}\left[1, e^{-j2\pi\mu^{\text{tx}}(\theta)},\ldots,e^{-j2\pi(N_{\text{tx}}-1)\mu^{\text{tx}}(\theta)}\right]^T,$$

where $\mu^{\text{tx}}(\theta) = d_{\text{tx}}\cos(\theta)/\lambda$, d_{tx} is the transmit antenna spacing, and λ is the wavelength. Similarly, $\mu^{\text{rx}}(\theta) = d_{\text{rx}}\cos(\theta)/\lambda$ and d_{rx} is receive antenna spacing. Lastly, $\alpha_{c,l}(t) = \bar{\alpha}_{c,l}\exp(j2\pi f_D t\cos(\omega_{c,l}))$, where $f_D = v/\lambda$ is the maximum Doppler shift, v is the speed of the UE that moves at an angle θ_v, $\bar{\alpha}_{c,l}$ is a circularly symmetric complex Gaussian RV with zero mean and variance γ_c (which is the relative power of the c^{th} cluster), and $\omega_{c,l} = \theta^{\text{rx}}_{c,l} - \theta_v$.

At time t, the beam gain $g_{i,p}(t)$ between the i^{th} transmit beam, which points in the direction $\theta^{\text{tx}}_i = \pi(i-1)/B_{\text{BS}}$ relative to the BS, and the p^{th} receive beam, which points in the direction $\theta^{\text{rx}}_p = \pi(p-1)/B_{\text{UE}}$ relative to the UE, equals

$$g_{i,p}(t) = |\mathbf{u}^\dagger_{\text{tx}}(\theta^{\text{tx}}_i)\mathbf{H}(t,\psi(t))\mathbf{u}_{\text{rx}}(\theta^{\text{rx}}_p)|. \quad (2)$$

Its power correlation coefficient $\rho_{i,p}(t,t+\tau)$ is defined as

$$\rho_{i,p}(t,t+\tau) \triangleq \frac{\mathbb{E}\left[g^2_{i,p}(t)\,g^2_{i,p}(t+\tau)\right] - \Omega_{i,p}(t)\,\Omega_{i,p}(t+\tau)}{\sqrt{\mathrm{Var}(g^2_{i,p}(t))\mathrm{Var}(g^2_{i,p}(t+\tau))}}. \quad (3)$$

The AoA $\theta^{\text{rx}}_{c,l}$ of path l of cluster c is a Gaussian RV that is wrapped over an interval of 2π radians. The Gaussian mean is $\bar{\theta}_{\text{AoA},c}$ and standard deviation is $\sigma_{AoA,c}$. Similarly, the AoD $\theta^{\text{tx}}_{c,l}$ is also a wrapped Gaussian RV with mean $\bar{\theta}_{\text{AoD},c}$ and standard deviation $\sigma_{\text{AoD},c}$. In SCM, the angular spread parameters $\sigma_{\text{AoA},c}$ and $\sigma_{AoD,c}$ are themselves exponential RVs with means ξ_{AoA} and ξ_{AoD}, respectively.

III. MBN Model for SCM's Time-Varying Channel

We develop an analytically tractable, accurate model for the joint statistics of the beam gains $g_{i,p}(t)$ and $g_{i,p}(t+\tau)$ obtained from SCM, where τ is the time lag. We define the normalized RVs $X_1 = g_{i,p}(t)/\sqrt{\Omega_{i,p}(t)}$ and $X_2 = g_{i,p}(t+\tau)/\sqrt{\Omega_{i,p}(t+\tau)}$, where $\Omega_{i,p}(t)$ is the mean beam power at time t.

A. When $\rho_{i,p}(t,t+\tau) \geq 0$

We propose modeling the bivariate PDF of X_1 and X_2 using the bivariate Nakagami-m model as follows [8]

$$f_{X_1,X_2}(x_1,x_2) = \frac{4m^{m+1}x_1^m x_2^m\left[1-\rho_{i,p}(t,t+\tau)\right]^{-1}}{\Gamma(m)\left(\rho_{i,p}(t,t+\tau)\right)^{\frac{m-1}{2}}} \times\exp\left[\frac{-m(x_1^2+x_2^2)}{1-\rho_{i,p}(t,t+\tau)}\right]I_{m-1}\left(\frac{2mx_1x_2\sqrt{\rho_{i,p}(t,t+\tau)}}{1-\rho_{i,p}(t,t+\tau)}\right), \quad (4)$$

where m is the Nakagami parameter and $I_m(.)$ denotes the modified Bessel function of the first kind of order m [9, (9.6.19)]. As per the maximum likelihood estimate given in [10], we set

$$m = \Omega^2_{i,p}(t)/\mathrm{Var}(g^2_{i,p}(t)). \quad (5)$$

B. When $\rho_{i,p}(t,t+\tau) < 0$

The bivariate Nakagami-m PDF is not defined for $\rho_{i,p}(t,t+\tau) < 0$. Therefore, an alternate model is needed. We first make two numerical observations from SCM and then develop the alternate model.

Figure 1 plots the level-set contours of the empirical bivariate PDF of the RVs X_1 and X_2 for $\tau = 17$ ms and 23 ms at $t = 20$ ms. The power correlation coefficients for these two lags turn out to be -0.81 and 0.83, respectively. They have approximately the same absolute value but opposite signs. The plots are generated from $100,000$ traces of gains of all beam pairs for $B_{\text{BS}} = 18$, $B_{\text{UE}} = 18$, $N_{\text{tx}} = N_{\text{rx}} = 20$, $d_{\text{rx}} = d_{\text{tx}} = 0.25\lambda$, $v = 2$ m/s, and carrier frequency of 28 GHz. The SCM parameters are $K = 3$, $\xi_{\text{AoD}} = 10.2°$, $\xi_{\text{AoD}} = 15.5°$, $C = 4$,

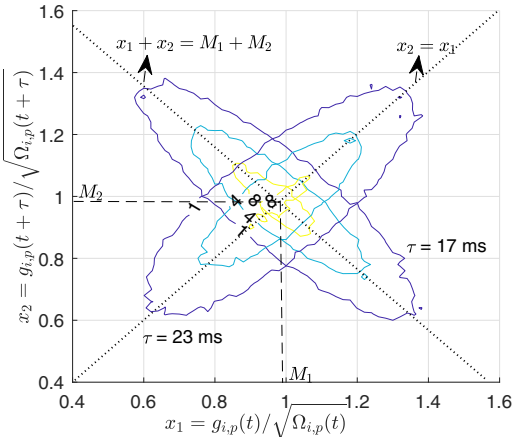

Fig. 1. Level-set contour plot of the empirical bivariate PDF of RVs X_1 and X_2 for $\tau = 17$ ms and 23 ms with $\rho_{i,p}(t, t+\tau) = -0.83$ and 0.81, respectively, at $\psi'(t) = 60°$/s ($K = 3$, $\xi_{\text{AoD}} = 10.2°$, $\xi_{\text{AoA}} = 15.5°$, $C = 4$, and $L = 20$, $t = 20$ ms). The PDF levels are 1, 4, and 8.

$L = 20$, and $\theta_v = 90°$, and the UE orientation change rate is $\psi'(t) = 60°$/s [4]. Each trace consists of 120 samples that are spaced 1 ms apart. We make the following observations, which hold for other parameter settings as well.

Numerical Observation 1: *The level-set contours for the positive power correlation coefficient are concentric, and so are those for the negative power correlation coefficient. Furthermore, all the level-set contours share the same center.*

Numerical Observation 2: *The major axes of the level-set contours for the positive and negative power correlation coefficients are perpendicular to each other.*

Explanation: $f_{X_1,X_2}(x_1, x_2)$ in (4) is a symmetric function of the variables x_1 and x_2. The positive correlation coefficient implies that the major axis of the contours has a positive slope. To ensure symmetry, it must be a 45° line. Thus, the major axis is $x_1 = x_2$.

In Numerical Observation 1, the center $\mathbf{c} = (M_1, M_2)$ is the point at which the bivariate Nakagami-m PDF is maximized. It is the solution of $\frac{\partial}{\partial x_1} f_{x_1,x_2}(x_1, x_2) = 0$ and $\frac{\partial}{\partial x_2} f_{x_1,x_2}(x_1, x_2) = 0$. When $\rho_{i,p}(t, t+\tau) > 0$, these are non-linear coupled equations without a closed-form solution. However, we have numerically observed that $\mathbf{c}$ is insensitive to $\rho_{i,p}(t, t+\tau)$.[1] Thus, it is the same as that for $\rho_{i,p}(t, t+\tau) = 0$. In this case, M_1 is the value of x_1 at which the marginal Nakagami-m PDF $f_{X_1}(x_1)$ is maximized. It equals $M_1 = \sqrt{(2m-1)/(2m)}$ [8]. Similarly, $M_2 = \sqrt{(2m-1)/(2m)}$.

For the negative correlation coefficient, we expect the bivariate PDF to remain a symmetric function of x_1 and x_2. The negative correlation implies a negative slope. This coupled with the symmetry and common center implies that the major axis is a 135°-line that passes through the point $\left(\sqrt{\frac{2m-1}{2m}}, \sqrt{\frac{2m-1}{2m}}\right)$. Thus, it is perpendicular to the line $x_2 = x_1$. After accounting for the fact that it passes through $\mathbf{c}$, the major axis is given by $x_2 = 2\sqrt{\frac{2m-1}{2m}} - x_1$.

Using an affine transformation of variables that satisfies the two observations, the bivariate PDF $\tilde{f}_{X_1,X_2}(x_1, x_2)$ equals

$$\tilde{f}_{X_1,X_2}(x_1, x_2) = \frac{4m^{m+1}(a - x_1)^m x_2^m}{\zeta(m, 2(2m-1))(1-\rho)\rho^{\frac{m-1}{2}}} \times \exp\left[\frac{-m\left((a-x_1)^2 + x_2^2\right)}{1-\rho}\right] I_{m-1}\left(\frac{2m\sqrt{\rho}(a-x_1)x_2}{1-\rho}\right), \quad \text{for } 0 \le x_1 \le a, x_2 \ge 0, \quad (6)$$

where $a = \sqrt{2(2m-1)/m}$, $\zeta(\cdot,\cdot)$ is the incomplete gamma function [11, (8.350.1)], and $\rho > 0$ is a parameter that affects correlation. The incomplete gamma function arises because of finite range of the PDF. The power correlation coefficient turns out to be approximately $-\rho$.

C. $\Omega_{i,p}(t)$ and $\rho_{i,p}(t, t+\tau)$ in Terms of SCM Parameters

The p^{th} receive beam directional coefficient at the UE $Z_p^{\text{rx}}(\theta) = \mathbf{u}_{\text{rx}}^\dagger(\theta_p^{\text{tx}})\mathbf{u}_{\text{rx}}(\theta)$ in the direction θ is given by

$$Z_p^{\text{rx}}(\theta) = \frac{1}{N_{\text{rx}}} \exp\left(-j(N_{\text{rx}}-1)\pi\left[\mu^{\text{rx}}(\theta) - \mu^{\text{rx}}\left(\theta_p^{\text{rx}}\right)\right]\right) \times \frac{\sin\left(N_{\text{rx}}\pi\left[\mu^{\text{rx}}(\theta) - \mu^{\text{rx}}\left(\theta_p^{\text{rx}}\right)\right]\right)}{\sin\left(\pi\left[\mu^{\text{rx}}(\theta) - \mu^{\text{rx}}\left(\theta_p^{\text{rx}}\right)\right]\right)}. \quad (7)$$

It follows that

$$\left|Z_p^{\text{rx}}(\theta)\right|^2 = \frac{1}{N_{\text{rx}}^2} \frac{\sin^2\left(N_{\text{rx}}\pi\left[\mu^{\text{rx}}(\theta) - \mu^{\text{rx}}\left(\theta_p^{\text{rx}}\right)\right]\right)}{\sin^2\left(\pi\left[\mu^{\text{rx}}(\theta) - \mu^{\text{rx}}\left(\theta_p^{\text{rx}}\right)\right]\right)}. \quad (8)$$

Similarly, for the i^{th} transmit beam, the directional coefficient $Z_i^{\text{tx}}(\theta) = \mathbf{u}_{\text{tx}}^\dagger(\theta_i^{\text{tx}})\mathbf{u}_{\text{tx}}(\theta)$ in the direction θ is

$$\left|Z_i^{\text{tx}}(\theta)\right|^2 = \frac{1}{N_{\text{tx}}^2} \frac{\sin^2\left(N_{\text{tx}}\pi\left[\mu^{\text{tx}}(\theta) - \mu^{\text{tx}}\left(\theta_i^{\text{tx}}\right)\right]\right)}{\sin^2\left(\pi\left[\mu^{\text{tx}}(\theta) - \mu^{\text{tx}}\left(\theta_i^{\text{tx}}\right)\right]\right)}. \quad (9)$$

In the following results, we skip derivations to conserve space.

1) Mean Beam Power $\Omega_{i,p}(t) = \mathbb{E}\left[g_{i,p}^2(t)\right]$: It is given by

$$\Omega_{i,p}(t) = \frac{\Lambda}{K+1} \sum_{c=1}^{C} \gamma_c \bar{G}_{p,c}^{\text{rx}}(t) \bar{G}_{i,c}^{\text{tx}}(t) + \frac{K\Lambda}{K+1} \left|Z_p^{\text{rx}}\left(\theta_{\text{LoS}}^{\text{rx}} + \psi(t)\right)\right|^2 \left|Z_i^{\text{tx}}\left(\theta_{\text{LoS}}^{\text{tx}}\right)\right|^2, \quad (10)$$

where $\bar{G}_{i,c}^{\text{tx}}(t) = \sum_{q=1}^{\text{GH}} w_q \left|Z_i^{\text{tx}}\left(\sqrt{2}\sigma_{\text{AoD},c}x_q + \bar{\theta}_{\text{AoD},c}\right)\right|^2/\sqrt{\pi}$, $\bar{G}_{p,c}^{\text{rx}}(t) = \sum_{q=1}^{\text{GH}} w_q \left|Z_p^{\text{rx}}\left(\sqrt{2}\sigma_{\text{AoA},c}x_q + \bar{\theta}_{\text{AoA},c} + \psi(t)\right)\right|^2/\sqrt{\pi}$, w_q and x_q are the q^{th} Gauss-Hermite (GH) weight and abscissa, respectively, for $1 \le q \le \text{GH}$ [9, (25.4.46)].

[1] Over a wide range of values of $\rho_{i,p}(t, t+\tau)$, the two elements of $\mathbf{c}$ vary by atmost 0.1% from those at $\rho_{i,p}(t, t+\tau) = 0$.

2) Power Correlation Coefficient $\rho_{i,p}(t,t+\tau)$: In (3), the denominator term $\mathrm{Var}(g_{i,p}^2(t))$ is given by

$$\begin{aligned}\mathrm{Var}(g_{i,p}^2(t)) = &\frac{2\Lambda^2}{L(K+1)^2}\left(\sum_{c_1=1}^{C}\gamma_{c_1}^2 F_{p,c_1}^{\mathrm{rx}}(t)F_{i,c_1}^{\mathrm{tx}}(t)\right.\\ &+2(L-1)\sum_{c_1=1}^{C}\gamma_{c_1}^2\left(\bar{G}_{p,c_1}^{\mathrm{rx}}(t)\right)^2\left(\bar{G}_{i,c_1}^{\mathrm{tx}}(t)\right)^2\\ &+2L\left[\sum_{c_1=1}^{C}\gamma_{c_1}\bar{G}_{p,c_1}^{\mathrm{rx}}(t)\bar{G}_{i,c_1}^{\mathrm{tx}}(t)\right]\left.\sum_{c_2=1,c_2\neq c_1}^{C}\gamma_{c_2}\bar{G}_{p,c_2}^{\mathrm{rx}}(t)\bar{G}_{i,c_2}^{\mathrm{tx}}(t)\right)\\ &+\frac{2K\Lambda^2\left|Z_i^{\mathrm{tx}}\left(\theta_{\mathrm{LoS}}^{\mathrm{tx}}\right)\right|^2\left|Z_p^{\mathrm{rx}}\left(\theta_{\mathrm{LoS}}^{\mathrm{rx}}+\psi(t)\right)\right|^2}{(K+1)^2}\sum_{c_1=1}^{C}\gamma_{c_1}\bar{G}_{p,c_1}^{\mathrm{rx}}(t)\bar{G}_{i,c_1}^{\mathrm{tx}}(t),\end{aligned} \tag{11}$$

where $F_{i,c}^{\mathrm{tx}}(t)=\sum_{q=1}^{\mathsf{GH}}w_q\left|Z_i^{\mathrm{tx}}\left(\sqrt{2}\sigma_{\mathrm{AoD},c}x_q+\bar{\theta}_{\mathrm{AoD},c}\right)\right|^4/\sqrt{\pi}$ and $F_{p,c}^{\mathrm{rx}}(t)=\sum_{q=1}^{\mathsf{GH}}w_q\left|Z_p^{\mathrm{rx}}\left(\sqrt{2}\sigma_{\mathrm{AoA},c}x_q+\bar{\theta}_{\mathrm{AoA},c}+\psi(t)\right)\right|^4/\sqrt{\pi}$. Replacing t with $t+\tau$ yields $\mathrm{Var}(g_{i,p}^2(t+\tau))$.

In (3), the numerator $\mathbb{E}\left[g_{i,p}^2(t)\,g_{i,p}^2(t+\tau)\right]$ equals

$$\begin{aligned}\mathbb{E}\left[g_{i,p}^2(t)\,g_{i,p}^2(t+\tau)\right] = &\,T_{i,p}^{\mathrm{NLoS}}(t,\tau)+T_{i,p}^{\mathrm{LoS}}(t,\tau)\\ &+T_{i,p}^{\mathrm{LoS,NLoS}}(t,\tau).\end{aligned} \tag{12}$$

Here, $T_{i,p}^{\mathrm{NLoS}}(t,\tau)$ captures the non-line-of-sight (NLoS) term cross-products:

$$\begin{aligned}T_{i,p}^{\mathrm{NLoS}}(t,\tau) = &\\ &\frac{\Lambda^2}{L(K+1)^2}\left[2\sum_{c_1=1}^{C}\gamma_{c_1}^2\bar{G}_{p,c_1}^{\mathrm{rx}}(t)F_{i,c_1}^{\mathrm{tx}}(t)\bar{G}_{p,c_1}^{\mathrm{rx}}(t+\tau)\right.\\ &+L\left[\sum_{c_1=1}^{C}\gamma_{c_1}\bar{G}_{p,c_1}^{\mathrm{rx}}(t)\bar{G}_{i,c_1}^{\mathrm{tx}}(t)\right]\sum_{c_2=1,c_2\neq c_1}^{C}\gamma_{c_2}\bar{G}_{p,c_2}^{\mathrm{rx}}(t+\tau)\bar{G}_{i,c_2}^{\mathrm{tx}}(t)\\ &+(L-1)\sum_{c_1=1}^{C}\gamma_{c_1}^2\bar{G}_{p,c_1}^{\mathrm{rx}}(t)\left(\bar{G}_{i,c_1}^{\mathrm{tx}}(t)\right)^2\bar{G}_{p,c_1}^{\mathrm{rx}}(t+\tau)\\ &+L\left[\sum_{c_1=1}^{C}\gamma_{c_1}\Theta_{c_1}^{\mathrm{rx}}(t,\tau)\bar{G}_{i,c_1}^{\mathrm{tx}}(t)\right]\sum_{c_2=1,c_2\neq c_1}^{C}\gamma_{c_2}\left(\Theta_{c_2}^{\mathrm{rx}}(t,\tau)\right)^*\bar{G}_{i,c_2}^{\mathrm{tx}}(t)\\ &\left.+(L-1)\sum_{c_1=1}^{C}\gamma_{c_1}^2\Theta_{c_1}^{\mathrm{rx}}(t,\tau)\left(\bar{G}_{i,c_1}^{\mathrm{tx}}(t)\right)^2\left(\Theta_{c_1}^{\mathrm{rx}}(t,\tau)\right)^*\right],\end{aligned} \tag{13}$$

where

$$\begin{aligned}\Theta_c^{\mathrm{rx}}(t,\tau) = &\frac{1}{\sqrt{\pi}}\sum_{q=1}^{\mathsf{GH}}w_q Z_p^{\mathrm{rx}}\left(\sqrt{2}\sigma_{\mathrm{AoA},c}x_q+\bar{\theta}_{\mathrm{AoA},c}+\psi(t)\right)\\ &\times\left(Z_p^{\mathrm{rx}}\left(\sqrt{2}\sigma_{\mathrm{AoA},c}x_q+\bar{\theta}_{\mathrm{AoA},c}+\psi(t+\tau)\right)\right)^*\\ &\times e^{4\pi jtf_D\sin\left(\sqrt{2}\sigma_{\mathrm{AoA},c}x_q+\bar{\theta}_{\mathrm{AoA},c}+\frac{\psi(t)+\psi(t+\tau)}{2}-\theta_v\right)\sin\left(\frac{\psi(t+\tau)-\psi(t)}{2}\right)}\\ &\times e^{-2\pi j\tau f_D\cos\left(\sqrt{2}\sigma_{\mathrm{AoA},c}x_q+\bar{\theta}_{\mathrm{AoA},c}+\psi(t+\tau)-\theta_v\right)}.\end{aligned} \tag{14}$$

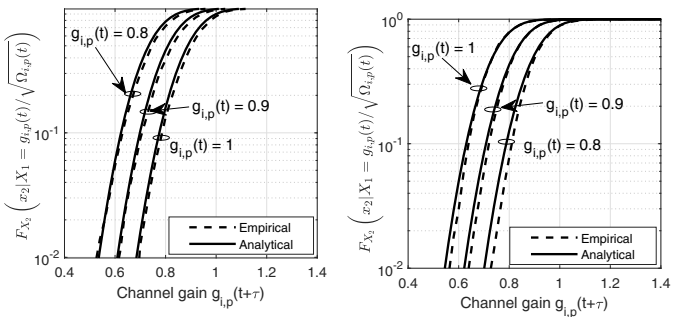

(a) $\rho_{i,p}(t,t+\tau)=0.81$ (b) $\rho_{i,p}(t,t+\tau)=-0.83$

Fig. 2. Verification of the MBN model: Conditional CDF $F_{X_2}\left(x_2|X_1=g_{i,p}(t)/\sqrt{\Omega_{i,p}(t)}\right)$ for positive and negative power correlation coefficients ($t=20$ ms, $\psi'(t)=60°$/s, $K=3$, $\xi_{\mathrm{AoD}}=10.2°$, $\xi_{\mathrm{AoA}}=15.5°$, $C=4$, and $L=20$).

$T_{i,p}^{\mathrm{LoS}}(t,\tau)$ captures the LoS term cross-products:

$$\begin{aligned}T_{i,p}^{\mathrm{LoS}}(t,\tau) = &\frac{K^2\Lambda^2}{(K+1)^2}\left|Z_p^{\mathrm{rx}}\left(\theta_{\mathrm{LoS}}^{\mathrm{rx}}+\psi(t)\right)\right|^2\\ &\times\left|Z_p^{\mathrm{rx}}\left(\theta_{\mathrm{LoS}}^{\mathrm{rx}}+\psi(t+\tau)\right)\right|^2\left|Z_i^{\mathrm{tx}}\left(\theta_{\mathrm{LoS}}^{\mathrm{tx}}\right)\right|^4.\end{aligned} \tag{15}$$

$T_{i,p}^{\mathrm{LoS,NLoS}}(t,\tau)$ captures LoS and NLoS term cross-products:

$$\begin{aligned}T_{i,p}^{\mathrm{LoS,NLoS}}(t,\tau) = &\frac{K\Lambda^2\left|Z_i^{\mathrm{tx}}\left(\theta_{\mathrm{LoS}}^{\mathrm{tx}}\right)\right|^2}{(K+1)^2}\\ &\times\left[\left(\sum_{c=1}^{C}\gamma_c\bar{G}_{p,c}^{\mathrm{rx}}(t)\bar{G}_{i,c}^{\mathrm{tx}}(t)\right)\left|Z_p^{\mathrm{rx}}\left(\theta_{\mathrm{LoS}}^{\mathrm{rx}}+\psi(t+\tau)\right)\right|^2\right.\\ &+\left(\sum_{c=1}^{C}\gamma_c\bar{G}_{p,c}^{\mathrm{rx}}(t+\tau)\bar{G}_{i,c}^{\mathrm{tx}}(t)\right)\left|Z_p^{\mathrm{rx}}\left(\theta_{\mathrm{LoS}}^{\mathrm{rx}}+\psi(t)\right)\right|^2\\ &+2\Re\left(\sum_{c=1}^{C}\gamma_c\Theta_c^{\mathrm{rx}}(t,\tau)\bar{G}_{i,c}^{\mathrm{tx}}(t)\right)\\ &\left.\times\left(Z_p^{\mathrm{rx}}\left(\theta_{\mathrm{LoS}}^{\mathrm{rx}}+\psi(t)\right)\right)^*Z_p^{\mathrm{rx}}\left(\theta_{\mathrm{LoS}}^{\mathrm{rx}}+\psi(t+\tau)\right)\right].\end{aligned} \tag{16}$$

D. MBN Model Verification

For different values of $g_{i,p}(t)$, Figure 2a plots the conditional CDF $F_{X_2}\left(x_2|X_1=g_{i,p}(t)/\sqrt{\Omega_{i,p}(t)}\right)$ for $\rho_{i,p}(t,t+\tau)=0.81$. Figure 2b does the same for $\rho_{i,p}(t,t+\tau)=-0.83$. We observe a good match over a three orders of magnitude range between the empirically obtained conditional CDF and the one derived from the bivariate PDFs in (4) and (6). In Figure 2a, the conditional CDF shifts to the right as $g_{i,p}(t)$ increases because $\rho_{i,p}(t,t+\tau)$ is positive. On the other hand, in Figure 2b, the reverse is true because $\rho_{i,p}(t,t+\tau)$ is negative.

IV. Application of MBN Model to Beam Selection

We consider a general measurement scheme, which is illustrated in Figure 3. Time is divided into beam measurement cycles. Each cycle is of duration T_{meas} and consists of $S<B_{\mathrm{UE}}$ pilot bursts. Each pilot burst consists of B_{BS} pilots and is of duration T_{p}. The UE measures all the B_{BS} pilots in a pilot burst

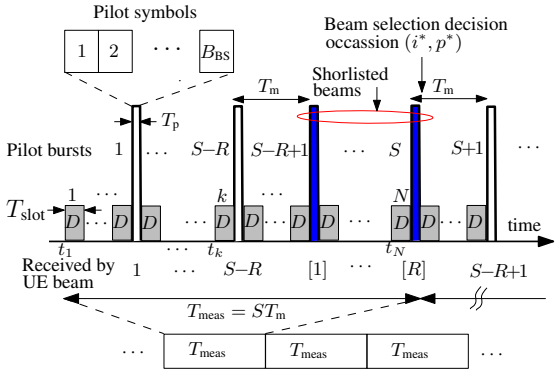

Fig. 3. Model for beam measurement, selection, and data transmission

in a sequential order with one receive beam. Thus, SB_{BS} beam pairs are measured in a beam measurement cycle.

To enable exploitation and exploration, the UE receives with R shortlisted beams that had the largest beam gains in the previous measurement cycle. These are denoted by $[1], \ldots, [R]$ in the figure. The other $S-R$ receive beams are drawn in a sequential order from the remaining $B_{\text{UE}} - R$ receive beams. When R is increased, more shortlisted beams are measured but fewer other beams are measured.

Data transmission also occurs over the duration of a measurement cycle. It occurs in N slots each of duration T_{slot}. These are denoted by D in the figure. The kth slot starts at time t_k. In compliance with the 5G standard, the BS can adapt its rate in each slot [5]. However, it can change its transmit beam only once in a cycle because of constraints on how often a UE can feed back its measurements. At the end of each measurement cycle, the UE selects the beam pair (i^*, p^*), which is used to transmit and receive data in the next cycle.

In general, let the UE measure the beam pair (i,p) at time $T_{i,p}$ and let the corresponding beam gain be $g_{i,p}(T_{i,p})$. Then, given the previous measurements, the expected SNR at the time t at which the beam is selected is equal to $P_{\text{tx}} d_{i,p}(t)/\sigma^2$, where

$$d_{i,p}(t) = \mathbb{E}_{X_2}\left[g_{i,p}^2(t) \,\middle|\, X_1 = g_{i,p}(T_{i,p}) / \sqrt{\Omega_{i,p}(T_{i,p})} \right]. \tag{17}$$

Using the MBN model, $d_{i,p}(t)$ is given in closed-form as follows:

a) $\rho_{i,p}(t) \geq 0$*:* From (4), using the conditional PDF $f_{X_2}\left(x_2 | x_1 = g_{i,p}(T_{i,p}) / \sqrt{\Omega_{i,p}(T_{i,p})}\right)$ and the identity $\int_0^\infty r_2^{m+2} e^{-\delta r_2^2} I_{m-1}(\nu r_2)\, dr_2 = e^{-\frac{\nu^2}{4\delta}} \frac{\nu^{m-1}(\nu^2 + 4\delta m)}{(2\delta)^{m+2}}$ [11, (6.631.1)] to evaluate the conditional expectation, we get

$$d_{i,p}(t) = \frac{\Omega_{i,p}(t)}{\Omega_{i,p}(T_{i,p})} \left[(1 - \rho_{i,p}(t))\, \Omega_{i,p}(T_{i,p}) + \rho_{i,p}(t)\, g_{i,p}^2(T_{i,p}) \right]. \tag{18}$$

b) $\rho_{i,p}(t) < 0$*:* Along similar lines as above, from the bivariate PDF in (6), we can show that

$$d_{i,p}(t) = \frac{\Omega_{i,p}(t)}{\Omega_{i,p}(T_{i,p})} \left[(1 - |\rho_{i,p}(t)|)\, \Omega_{i,p}(T_{i,p}) + |\rho_{i,p}(t)| \left(a - g_{i,p}(T_{i,p})\right)^2 \right]. \tag{19}$$

For $\rho_{i,p}(t) \geq 0$, when $g_{i,p}(T_{i,p})$ is large, the odds that the beam pair (i,p) will be selected increase. The reverse is true when $\rho_{i,p}(t) < 0$. As $|\rho_{i,p}(t)|$ decreases from 1 to 0, the weightage for the term that depends on $g_{i,p}(T_{i,p})$ decreases.

Note from (10) and (3) that $\Omega_{i,p}(t)$ and $\rho_{i,p}(t, t+\tau)$ can be calculated from the orientation $\psi(t)$ of the UE and the Doppler shift f_D. The orientation can be tracked and predicted using orientation sensors installed in the UE [2], [3] and f_D using level-crossing rate or the channel covariance methods.

Prediction-Based Rule (PBR): Using the above results, we propose the following rule that calculates the expected data rate from using the predicted SNRs using the Shannon capacity formula:

$$(i^*, p^*) = \underset{i \in \mathcal{B}_{\text{BS}}, p \in \mathcal{B}_{\text{UE}}}{\arg\max} \left\{ \frac{1}{N} \sum_{k=1}^{N} \log_2 \left(1 + \frac{P_{\text{tx}} d_{i,p}(t_k)}{\sigma^2} \right) \right\}. \tag{20}$$

This captures the rate adaptation by the BS from one slot to another and also the 5G constraint that it must use the same beam to transmit data in a measurement cycle.

A. Numerical Results and Benchmarking

We illustrate the results for $B_{\text{BS}} = 18$, $B_{\text{UE}} = 18$, $N_{\text{tx}} = N_{\text{rx}} = 20$, $d_{\text{rx}} = d_{\text{tx}} = 0.25\lambda$, $v = 3.85$ kmph, and carrier frequency of 28 GHz. Let $\eta = G_{\max}^{\text{tx}} G_{\max}^{\text{rx}} P_{\text{tx}} \Lambda / \sigma^2$ denote the peak SNR when the transmit and receive beams are aligned, where $G_{\max}^{\text{tx}} = 13$ dB and $G_{\max}^{\text{rx}} = 13$ dB represent the peak transmit and receive beam gains, respectively. For SCM, the parameters are $K = 3$, $\xi_{\text{AoD}} = 10.2°$, $\xi_{\text{AoA}} = 15.5°$, $C = 4$, and $L = 20$. The beam measurement and data transmission parameters are $T_{\text{slot}} = 0.125$ ms and $T_{\text{p}} = 5.14 T_{\text{slot}}$. We set $S = 6$ and $T_{\text{m}} = 20$ ms. Thus, $T_{\text{meas}} = 120$ ms.

We benchmark PBR with the following rules:

- *Conventional Rule (CR) [5]–[7]:* It is given by

$$(i^*, p^*) = \underset{i \in \mathcal{B}_{\text{BS}}, p \in \mathcal{B}_{\text{UE}}}{\arg\max} \left\{ g_{i,p}^2(T_{i,p}) \right\}. \tag{21}$$

- *Non-Causal Genie-Aided Rule:* It is given by

$$(i^*, p^*) = \underset{i \in \mathcal{B}_{\text{BS}}, p \in \mathcal{B}_{\text{UE}}}{\arg\max} \left\{ \sum_{k=1}^{N} \log_2 \left(1 + \frac{P_{\text{tx}} g_{i,p}^2(t_k)}{\sigma^2} \right) \right\}. \tag{22}$$

  It requires the UE to know at the time of selection the gains for all the beams in the next N data slots. It provides an upper bound on the average rate achievable by any practical, causal rule.

Our results are computed from 30 SCM channel traces, which are generated using (1) given the value of $\psi'(t)$. Each trace is of

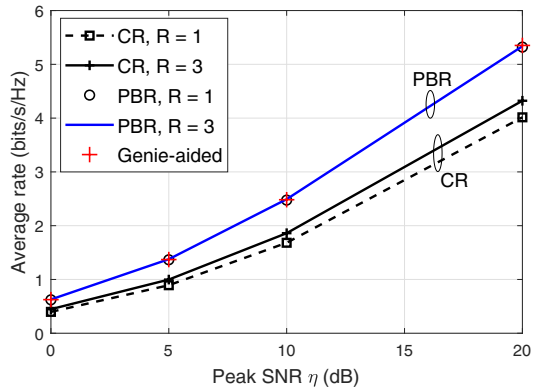

Fig. 4. Performance benchmarking of the average rates of the CR and PBR as a function of the peak SNR η ($\psi'(t) = 60°$/s).

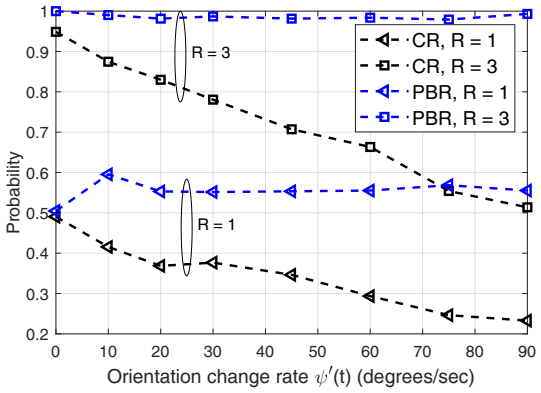

Fig. 5. Zoomed-in view of the top-R probability as a function of the UE orientation change rate $\psi'(t)$ for CR and PBR ($\eta = 20$ dB).

duration 12 s. We then use the beam selection rule to determine the transmit-receive beam pair.[2]

B. Numerical Results

Figure 4 compares the average rates of PBR, CR, and genie-aided rule as a function of the peak SNR η for $\psi'(t) = 60°$/s. The average rate of CR for $R = 1$ is greater than that for $R = 3$ for which the measurement cycle is longer. This shows the importance of controlling the training overhead. This is not the case for the PBR; the curves for $R = 1$ and 3 are now indistinguishable. PBR achieves a markedly higher average rate than CR; the gap between the two increases as η increases. PBR's average rate is close to that of the genie-aided rule.

To understand the above behavior, Figure 5 plots the top-R probability, which is the probability that the best beam is in the R shortlisted beams, as a function of the user orientation change rate $\psi'(t)$. The higher this probability, the better is the ability of the beam selection rule to shortlist the receive beams that are likely to be selected and measure their beam gains. This probability is always 100% for the genie-aided rule. For $R = 3$, as $\psi'(t)$ increases, the top-R probability markedly decreases for CR, while that of the PBR remains above 98%. The behavior is similar for $R = 1$, except for an increase when $\psi'(t)$ increases from 0°/s to 10°/s. This is because PBR is able to shortlist with a higher probability the beam towards which the UE is orienting itself. We do not observe this for $R = 3$ as the probability is close to one. The top-R probability is lower for $R = 1$ because the odds that the best beam pair will be shortlisted decrease.

[2]To compute $\bar{G}^{\text{rx}}_{p,c}(t)$, $\bar{G}^{\text{tx}}_{i,c}(t)$, $F^{\text{rx}}_{p,c}(t)$, and $F^{\text{tx}}_{i,c}(t)$, which are required by PBR, we use $\mathsf{GH} = 24$. To compute $\Theta^{\text{rx}}_{c}(t,\tau)$, which shows oscillatory behavior, we use $\mathsf{GH} = 8\tau f_D$, subject to a minimum of 24 terms and a maximum of 63 terms. The computed values are accurate to within 0.1%.

V. Conclusions

We proposed a novel and tractable MBN model for statistically characterizing the time-evolution of the non-stationary beam gains that arise in the widely used SCM. It accurately captured the impact of user orientation changes and applied to both positive and negatively correlated scenarios. It was accurate over a two order of magnitude range of beam gains.

With the help of MBN, we proposed a new beam selection rule for the practical scenario in which the beam gains of the different transmit-receive beam pairs were measured at different times and were outdated by different extents at the time the BS selected the beam pair. The rule markedly increased the odds that the best beam was shortlisted for measurement. Its data rate was much more than that of the conventional rule and indistinguishable from the non-causal genie-aided rule. It was also robust to UE orientation changes. An interesting avenue for research is to extend this work for wideband dual-polarized channels and model the correlation of gains across different beams.

References

[1] T. S. Rappaport, S. Sun, R. Mayzus, H. Zhao, Y. Azar, K. Wang, G. N. Wong, J. K. Schulz, M. Samimi, and F. Gutierrez, "Millimeter wave mobile communications for 5G cellular: It will work!" *IEEE Access*, vol. 1, pp. 335–349, May 2013.

[2] D. S. Shim, C. K. Yang, J. H. Kim, J. P. Han, and Y. S. Cho, "Application of motion sensors for beam-tracking of mobile stations in mmWave communication systems," *Sensors*, vol. 14, no. 10, pp. 19 622–19 638, Oct. 2014.

[3] A. K. R. Chavva, S. Khunteta, C. Lim, Y. Lee, J. Kim, and Y. Rashid, "Sensor intelligence based beam tracking for 5G mmwave systems: A practical approach," in *Proc. Globecom*, Dec. 2019, pp. 1–6.

[4] "Study on channel model for frequencies from 0.5 to 100 GHz," 3rd Generation Partnership Proj. (3GPP), TR 38.901, v16.1.0, 2019.

[5] M. Giordani, M. Polese, A. Roy, D. Castor, and M. Zorzi, "A tutorial on beam management for 3GPP NR at mmWave frequencies," *IEEE Commun. Surv. Tuts.*, vol. 21, no. 1, pp. 173–196, 4th Qtr. 2019.

[6] L. Wei, Q. Li, and G. Wu, "Exhaustive, iterative and hybrid initial access techniques in mmWave communications," in *Proc. WCNC*, Mar. 2017, pp. 1–6.

[7] Y. R. Li, B. Gao, X. Zhang, and K. Huang, "Beam management in millimeter-wave communications for 5G and beyond," *IEEE Access*, vol. 8, pp. 13 282–13 293, Jan. 2020.

[8] M. Nakagami, "The m-distribution—a general formula of intensity distribution of rapid fading," in *Statistical Methods in Radio Wave Propagation*, W. Hoffman, Ed. Pergamon, Jun. 1960, pp. 3–36.

[9] M. Abramowitz and I. Stegun, *Handbook of Mathematical Functions with Formulas, Graphs, and Mathematical Tables*, 9th ed. Dover, 1972.

[10] J. Cheng and N. C. Beaulieu, "Maximum-likelihood based estimation of the Nakagami-m parameter," *IEEE Commun. Lett.*, vol. 5, no. 3, pp. 101–103, Mar. 2001.

[11] L. S. Gradshteyn and L. M. Ryzhik, *Tables of Integrals, Series and Products*, 7th ed. Academic Press, 2007.